

**ORIGINAL RESEARCH PAPER**

## Catalytically Graphitized Electrospun Carbon Nanofibers Adorned with Nickel Nanoparticles for Catalysis Applications

A. M. Bazargan<sup>1\*</sup>, M. Esmailpour<sup>2</sup>, M. Keyanpour-rad<sup>3</sup>

<sup>1</sup>Department of Polymer Engineering and Color Technology, Amirkabir University of Technology, 15875-4413 Tehran, Iran

<sup>2</sup>Department of Materials Engineering, Isfahan University of Technology (IUT), Isfahan, 84156-83111, Iran

<sup>3</sup>Materials and Energy Research Center, P. O. Box 14155-4777, Tehran, Iran

### ARTICLE INFO.

Received 26/10/2015

Accepted 27/12/2015

Published online 01/01/2016

### KEYWORDS

Catalytic graphitization

Electrospinning

Graphitized nanofibers

Nickel nanoparticles

### ABSTRACT

Catalytically graphitized electrospun carbon nanofibers adorned uniformly with fine nickel nanoparticles were successfully prepared. The procedure was based on the electrospinning technique and the use of nickel precursor to create both graphitized nanofibers and nickel nanoparticles under a relatively low-temperature heat treatment. The X-ray diffraction and Raman results clearly proved catalytic graphitization of polymer-based carbon fibers in the presence of nickel catalyst. Taking the results from scanning and transmission electron microscopies and X-ray diffraction into account, it was inferred that during the heat treatment, nickel atoms have diffused through the nanofibers and formed fine nickel nanoparticles on the surface of graphitized nanofibers to make a well stabilized heterogeneous nanostructure. The results from Brunauer–Emmett–Teller technique also showed a high surface area value of 140.2 m<sup>2</sup>g<sup>-1</sup> for the obtained structure. All these attributes along with the fibrous and porous structure enable the product to serve as a potential candidate in the catalysis applications.

### INTRODUCTION

Supported metal catalysts are very important for energy and chemical industries to reduce consumption of raw materials and minimize waste production [1]. Supported nickel (Ni) catalysts have long been used in hydrogenation and dehydrogenation reactions and in steam reforming of hydrocarbons, due to their relatively high catalytic activity and cheapness [2]. Ni-based catalysts have also been ideally researched and used for the catalytic steam reforming of ethanol for hydrogen production due to the fact that as a clean and efficient energy, hydrogen is predicted to play an important role in future energy systems [3]. Thanks to their chemical inertness, controllable porosity and

surface chemistry and easy burning off, carbon materials have been successfully employed as catalyst support in multitude of hydrogenation, oxidation, hydrodesulphuration, hydrodenitrogenation and Fischer–Tropsch reactions [4]. Graphite is another standard carbon material widely employed in catalytic hydrodechlorination, hydrogenation, oxidation or ring transformation reactions [5].

Carbon nanofibers (CNFs) have attracted great research interest and have been employed in a number of catalytic reactions, such as Fischer–Tropsch, hydrogenation and ammonia synthesis reactions owing to combination of the most interesting properties such as high surface area and porosity, high mechanical strength, chemical inertness, and thermal stability [6, 7]. CNFs were recently produced by pyrolyzing

\*Corresponding author

Email address: [ambazargan@aut.ac.ir](mailto:ambazargan@aut.ac.ir)

Tel.: +98-9131147323

electrospun nanofibers from polyacrylonitrile [8-10] and from pitch [11] with typical diameters of few hundreds of nanometer and several microns, respectively.

Electrospinning is a powerful technique widely used for producing submicron fibers from polymer solutions [12]. This method bears nano-sized fibers which will be converted to CNFs through carbonization. The electrospun CNFs have a well-defined porous structure and high surface area compared to those obtained using traditional methods [13]. Moreover, other synthetic procedures employed to prepare these materials are quite complicated and they do not allow an adequate control over the textural properties [14].

Chambers et al. prepared supported Ni catalysts by incipient wetness of fumed  $\gamma$ -alumina, active carbon and vapor grown graphite nanofibers (GNFs) using a solution of Ni nitrate dissolved in deionized water and isobutyl alcohol. It was found that when the metal was dispersed on GNFs, the activity and selectivity of 1-butene and 1,3-butadiene hydrogenation were significantly altered in comparison with the catalysts supported on active carbon and  $\gamma$ -Al<sub>2</sub>O<sub>3</sub>. It was assumed that the strong interaction between metal nanoparticles and the p-electrons of the support medium was responsible for the difference of catalytic performance [15].

Baker et al. prepared vapor grown GNF-supported Ni catalysts by a standard incipient wetness technique. A survey was conducted about catalytic activity of Ni decorating GNFs in the gas-phase hydrogenation of light hydrocarbons at atmospheric pressure which exhibited higher activity in comparison with conventional support [16]. It has been proved that for obtaining a high dispersion and stability of the noble metal catalyst particles, the characteristics of the support are mainly the key factors. High crystallinity (resulting in proper electrical conductivity), relatively large surface area, and open and accessible porosity are mainly the commanding properties. Nevertheless, the synthesis of GNF-supported metal catalysts with high dispersion and high catalytic activity remains a challenge.

Here we introduce a simple and novel route to prepare highly dispersed Ni nanoparticles on catalytically graphitized electrospun carbon nanofibers (CGECNFs) with open and accessible porosity and high surface area. An impregnated solution is electrospun and the resulting composite fibers are undergone a relatively

low-temperature heat treatment which results in concurrent formation of graphitized nanofibers and Ni nanoparticles.

## MATERIALS AND METHODS

### *Preparation of CGECNF supported- Ni nanoparticles*

A 12 wt% polyacrylonitrile (PAN) solution was prepared by dissolving the predetermined amount of PAN (Mw = 80 kg.mol<sup>-1</sup>, Isfahan Polyacryle Co.) in dimethylformamide (DMF, Merck) under vigorous stirring at room temperature for 24 h. The PAN solution was then supplemented with Nickel(II) acetylacetonate (Ni(acac)<sub>2</sub>) in the proportion of 5:12 to PAN. The resulting solution was subsequently electrospun at the positive voltage of 11.5 kV with a constant feed rate of 0.5 cm<sup>3</sup> h<sup>-1</sup> and collection distance of 10 cm with the aid of the electrospinning setup used in our previous studies [17-19]. The electrospun nanofibers afterwards were stabilized in a tubular furnace at 230°C in air for 1h. The fibers were then heated at a rate of 3°C/min under N<sub>2</sub> atmosphere and were maintained at 800°C for 1 h, following at 1400°C for a period of 20 h. The experimental procedure has been schematically shown in Figure 1.

### *Characterizations*

The surface morphology of the samples was observed by a scanning electron microscope (SEM-S360 Cambridge) working at accelerating voltage of 20 kV. The average diameter of the fibers was appraised from the SEM images in the original magnification of 10 k, using ImageJ software [19]. A transmission electron microscope (TEM, Philips CM120 Netherland) was also used for further observation of the product under the accelerating voltage of 100 kV. Toward identifying the formed phases, X-ray diffraction (XRD) patterns were obtained using a Philips X-ray diffractometer (PW3710) with a graphite-monochromatized high intensity Cu K $\alpha$  radiation ( $\lambda=1.540598$  Å) operated at 30 kV and 25 mA within the range of  $2\theta = 20-50$  deg., with a step size of 0.02° and time per step of 100 sec. The mean interlayer spacing, d002, was determined from the position of the (002) peak applying Bragg's equation. The mean crystallite size, Lc was calculated from the (002) peak width using the Scherrer formula with K = 0.9 [20].

Raman spectrum was recorded by Almega Raman spectrometer with a 514.5 nm He-Ne laser line as the excitation source in the range of 600-2000 cm<sup>-1</sup>. The

specific surface area and pore size distribution of the product were evaluated using the Brunauer–Emmett–Teller (BET) method with N<sub>2</sub> adsorption/desorption at 77 K by Micromeritics (Gemini2375) in the relative pressure range of 0.05-1.00 and Belsorp adsorption/desorption data analysis software. Degassing of the samples was done at 75°C for 1 h.

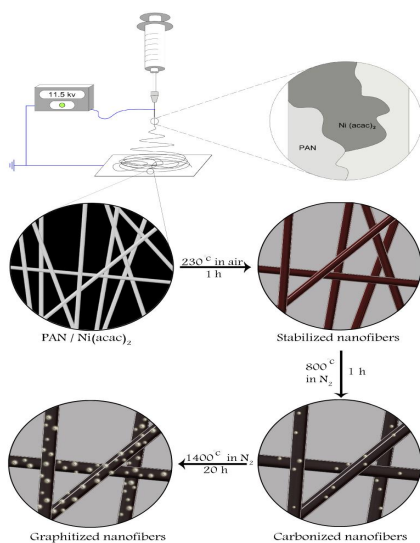


**Fig. 1.** Schematic of the experimental procedure used in the study.

## RESULTS AND DISCUSSION

Conversion of the PAN fiber precursor to graphite fiber involves three major steps; oxidative stabilization, carbonization and graphitization. Stabilization, which is done in atmosphere, changes the chemical structure of the PAN fibers to become thermally stable and do not melt during the subsequent heat treatment [21]. This process can be explained by involved chemical reactions which are cyclization, dehydrogenation, aromatization, oxidation and crosslinking resulting in the formation of fully aromatic cyclized structure shown in Fig. 2a, proposed by Houtz [22, 23]. During the carbonization and graphitization, the PAN fibers undergo heat treatment at a high temperature up to 800 - 3000°C which changes the PAN structure as illustrated in Fig. 2b. At this stage, a suitable catalyst can play a key role to reduce the activation energy required for graphitization and lower the graphitization temperature as well as improving the quality of the final product.

Fig. 3 shows the typical SEM and TEM images of

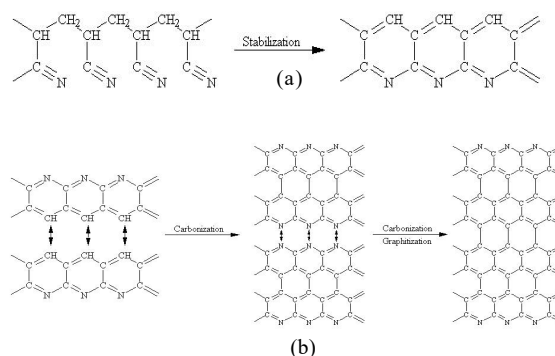
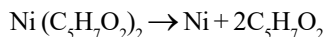


**Fig. 2.** a) Fully aromatic cyclized structure and b) structural changes of PAN precursor during the heat treatment

CGECNF-supported Ni nanoparticles. The images suggest that the sample possesses large area uniformity and an overall desired morphology along with being free of morphological defects. Image processing studies on the SEM images indicated an almost narrow range of variation for GNFs' diameter and estimated an average fiber diameter of  $160 \pm 12$  nm. The SEM images obviously depict that the Ni nanoparticles, the product of Ni(acac)<sub>2</sub> decomposition reaction, are well dispersed on the surface of GNF support and are in the diameter range of 40-60 nm. It is recognized that the dispersion of catalyst material within the support is one of the key factors affecting the catalytic reactivity and performance of the product, as it has been concluded in other studies [3, 24]. In the TEM micrograph (Fig. 3d), an individual GNF with the diameter of ~ 25 nm and Ni nanoparticles with the diameter of ~ 30 nm can be seen.

The thermal decomposition (pyrolysis) of Ni(acac)<sub>2</sub> in an inert atmosphere occurs through the following reaction at around 250 °C [25];



The formation of atomic Ni is due to the presence of inert atmosphere and carbon medium, a powerful reductant which hinders the formation of Ni oxide. The atomic Ni with radius of 1.25 Å can easily diffuse through the graphite hexagonal structure with c-axis spacing (d002) of 3.35 Å (for highly oriented pyrolytic graphite) [26], on condition that there are a concentration gradient, adequate time and thermal energy, under Fick's laws of diffusion. The Fick's first law (eq. 1) asserts that the diffusive flux goes from regions of high concentration to lower ones, with a

magnitude that is proportional to the concentration gradient. According to Fick's second law (eq. 2) which is employed in unsteady-state diffusion situations, time dependency of concentration changes is proportional to the second derivative of concentration.

$$J = -D \frac{\partial C}{\partial x} \quad (1)$$

$$\frac{\partial C}{\partial t} = D \left( \frac{\partial^2 C}{\partial x^2} \right) \quad (2)$$

$$D = D_0 \exp \left( \frac{-E}{RT} \right) \quad (3)$$

In the above equations,  $J$  is the diffusive flux,  $D$  is the diffusion coefficient,  $C$  is the concentration,  $X$  is the position of the atoms,  $t$  is time,  $D_0$  is the maximum diffusion coefficient,  $E$  is the activation energy for diffusion,  $R$  is the gas constant and  $T$  is the temperature [27].

On the basis of these criteria, the Ni atoms resulting from the pyrolysis of  $\text{Ni}(\text{acac})_2$  in an inert atmosphere, migrate from the bulk to the surface of GNFs due to the presence of Ni concentration gradient between the bulk and surface of GNFs and sustained heat treatment for 20 hours. This results in the formation and subsequent growth of Ni nanoparticles from the interface of Ni nanoparticles and GNFs as can be clearly seen in Fig. 3c. So, it can be deduced that the size of Ni nanoparticles can be controlled by heat treatment time and the temperature.

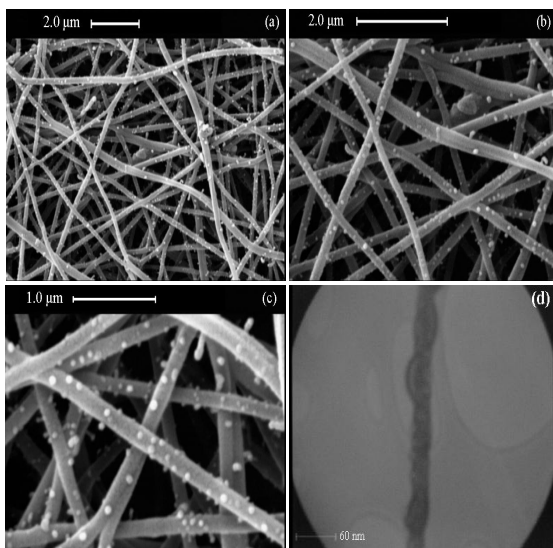


**Fig. 3.** SEM (a-c) and TEM (d) images of CGECNF-supported Ni nanoparticles

Fig. 4 displays the XRD pattern of the CGECNF-supported Ni nanoparticles. The predominant peak was identified to be at  $2\theta = 26.24^\circ$  corresponding to the diffraction of the (0 0 2) plane of the graphite structure with mean interlayer spacing,  $d_{002}$ , of 0.339 nm (which is very close to the 0.335 nm for single crystal hexagonal graphite) and mean crystallite size,  $L_c$ , of 6.77 nm (see Table 1) which give a clear indication of well-ordered and highly crystalline nature of these GNFs. The difference between the mean interlayer spacing and that of single crystal hexagonal graphite is probably attributable to the presence of H, O and N, and the presence of  $\text{sp}^3$  bonds [26, 28]. The peaks observed at approximately  $42^\circ$  and  $44^\circ$  diffraction angles, respectively ascribed to the diffraction of the (101) and (100) planes of the graphite structure in the resulted GNFs and the diffraction peak at  $2\theta = 45^\circ$  corresponding to Ni (111) can also be clearly seen [29].

Regarding the Scherrer formula,  $L_c = \frac{\lambda}{\Delta 2\theta \cos \theta}$ , and substituting the relevant parameters, the mean crystallite size of Ni nanoparticles ( $L_c$ ) was also calculated to be 24.6 nm which can be concluded that the Ni nanoparticles are generally composed of two or three Ni crystallites and are not single crystalline, comparing with the SEM image analysis results. The main diffraction peaks of NiO and Ni carbides were not detected in the XRD analysis.

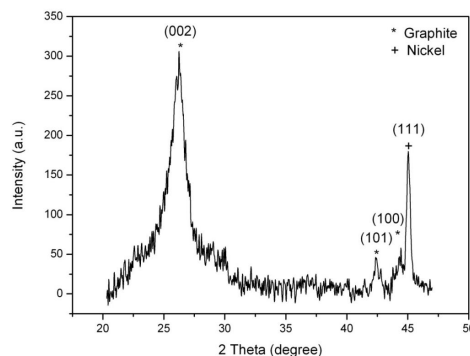


**Fig. 4.** The XRD pattern of the CGECNF-supported Ni nanoparticles

To confirm the outcome of XRD pattern, the crystalline structure of graphite was characterized by Raman spectroscopy and the result is presented in Fig. 5. Hexagonal crystal graphite structure shows a Raman active peak at  $1587 \text{ cm}^{-1}$  (G mode) corresponding to the graphitic band that is related to

**Table 1.** The structural parameters of CGECNF-supported Ni nanoparticles determined by XRD, Raman spectroscopy and BET technique

Raman					XRD					BET			Mean Pore Diameter
D-band position (cm <sup>-1</sup> )	G-band position (cm <sup>-1</sup> )	D-band FWHM (cm <sup>-1</sup> )	G-band FWHM (cm <sup>-1</sup> )	I <sub>D</sub> /I <sub>G</sub>	L <sub>a</sub> <sup>a</sup> (nm)	2θ (°)	d <sub>002</sub> (nm)	FWHM (deg)	L <sub>c</sub> (002) (nm)	S <sub>BET</sub> (m <sup>2</sup> g <sup>-1</sup> )	V <sub>p</sub> <sup>b</sup> (cm <sup>3</sup> g <sup>-1</sup> )	Mean Pore Diameter (nm)	
1344	1587	88	78	0.9	4.8	26.24	0.339	1.2	6.77	140.2	0.2	5.8	

the order of the sample, and a band around 1344 cm<sup>-1</sup> can be attributed to the D mode of disorder-induced scattering, which is due to imperfection or lack of hexagonal symmetry in the carbon structure. Thus, the ratio (R) of the peak intensity at 1344 cm<sup>-1</sup> (I<sub>D</sub>) to that at 1587 cm<sup>-1</sup> (I<sub>G</sub>) and the full width at half maximum intensity (FWHM) of the peaks are typical parameters to quantify the degree of disorder in carbon materials which are listed in table 1.

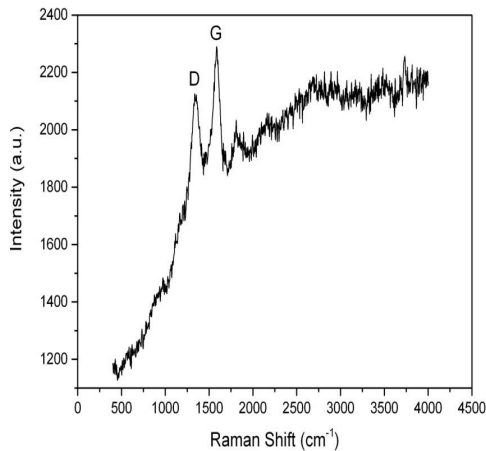


**Fig. 5.** The Raman spectrum of CGECNF-supported Ni nanoparticles.

The nitrogen adsorption/desorption isotherm of the CGECNF-supported Ni nanoparticles is shown in Fig. 6 and the associated BET surface area, total pore volume and the mean pore diameter values are given in table 1. The nitrogen adsorption/desorption isotherm is type II and exhibits a hysteresis loop associated to capillary condensation that signifies the existence of mesopores with the mean diameter of 5.8 nm. The BET

surface area of about 140 m<sup>2</sup>g<sup>-1</sup> is much larger than the values reported before for the GNF supported Ni particles [16], vapor grown CNF supported Ni catalysts [2],  $\alpha$ -alumina supported Ni particles [16], Ni catalysts supported on carbon nanospheres [6] and graphitized CNFs produced by the catalytic decomposition of natural gas [30]. The porous structure of nanofibrous support (with porosity of more than 90% [19]) along with the surface area of fine Ni nanoparticles and existence of tiny pores in the bulk and surface of GNFs, due to the evaporation of organic parts during heat treatment, are responsible for achieving such a high BET surface area.

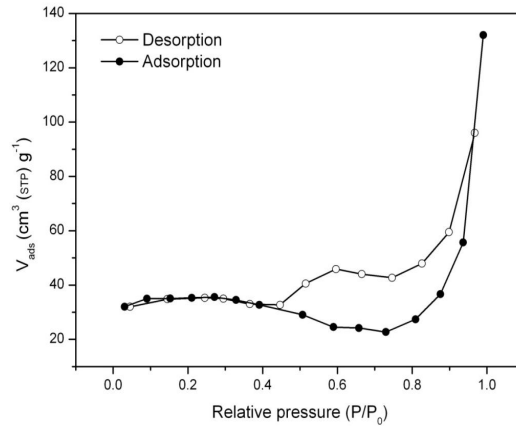


**Fig. 6.** The nitrogen adsorption/desorption isotherm of the CGECNF-supported Ni nanoparticles

## CONCLUSION

A simple route was reported to prepare fine Ni nanoparticles which were uniformly dispersed on the surface of CGECNF. The product was scrutinized with

an aid of the SEM, TEM, X-ray diffractometer, Raman spectroscopy and the BET technique to evaluate its quality and functionality. The results proved that the prepared heterogeneous nanostructure possesses large area uniformity and an overall desired morphology. It also enjoys a highly crystalline and well ordered graphite structure with a superior BET surface area of 140.2 m<sup>2</sup>/g.

#### ACKNOWLEDGMENTS

This work was supported by a grant from the Materials and Energy Research Center, No 728812. The authors are also thankful to Eng. Z. Bazargan for the graphical illustrations.

#### CONFLICT OF INTEREST

The authors declare that there are no conflicts of interest regarding the publication of this manuscript.

#### REFERENCES

- [1] M. K. Van der Lee, A. Jos van Dillen, H. Bitter Johannes, K. P. De Jong, *J. Am. Chem. Soc.* 127 (2005) 13573-13582.
- [2] C. Wang, J. Qiu, C. Liang, L. Xing, X. Yang, *Catal. Comm.* 9 (2008) 1749-1753.
- [3] C. Wu, P. T. Williams, *Environ. Sci. Technol.* 44 (2010) 5993-5998.
- [4] F. Coloma, A. S. Iveda-Escribano, J. L. G. Fierro, F. Rodríguez-Reinoso, *Appl. Catal. A: Gen.* 150 (1997) 165-183.
- [5] C. Amorim, G. Yuan, P. M. Patterson, M. A. Keane, *J. Catal.* 234 (2005) 268-281.
- [6] A. Nieto-Marquez, D. Toledano, J. C. Lazo, A. Romero, J. L. Valverde, *Appl. Catal. A: Gen.* 373 (2010) 192-200.
- [7] K. P. De Jong, J. W. Geus, *Catal. Rev. Sci. Eng.* 42 (2000) 481-510.
- [8] I. Chun, D. H. Reneker, H. Fong, X. Y. Fang, J. Dietzel, N. B. Tan, K. Kearns, *J. Adv. Mater.* 31 (1999) 36-41.
- [9] S. Sarkar, L. Zhai, *Mater. Express* 1 (2011) 18-29.
- [10] Y. Wang, S. Serrano, J. J. Santiago-Aviles, *Syn. Metals* 138 (2003) 423-427.
- [11] S. H. Park, C. Kim, K. S. Yang, *Syn. Metals* 143 (2004) 175-179.
- [12] T. Hyeon, S. Han, Y. Sung, K. Park, Y. Kim, *Angew. Chem. Int. Ed.* 42 (2003) 4352-4356.
- [13] S. Han, Y. Yun, K. Park, Y. Sung, T. Hyeon, *Adv. Mater.* 15 (2003) 1922-1925.
- [14] F. J. Maldonado-Hodar, C. Moreno-Castilla, J. Rivera-Utrilla, Y. Hanzawa, Y. Yamada, *Langmuir* 16 (2000) 4367-4373.
- [15] A. Chambers, T. Nemes, N. M. Rodriguez, R. T. K. Baker, *J. Phys. Chem. B* 102 (1998) 2251-2258.
- [16] C. Park, R. T. K. Baker, *J. Phys. Chem. B* 102 (1998) 5168-5177.
- [17] A. M. Bazargan, S. M. A. Fatemina, M. Esmailpour Ganji, M. A. Bahrevar, *Chem. Eng. J.* 155 (2009) 523-527.
- [18] M. Esmailpour Ganji, A. M. Bazargan, M. Keyanpour-rad, M. A. Bahrevar, *Func. Mater. Lett.* 3 (2010) 141-145.
- [19] A. M. Bazargan, M. Keyanpour-rad, F. A. Hesari, M. Esmailpour Ganji, *Desalination* 265 (2011) 148-152.
- [20] J. Bischof, B. J. Warren, *J. Appl. Phys.* 13 (1942) 364-372.
- [21] N. Yusof, A. F. Ismail, *J. Anal. Appl. Pyrol.* 93 (2012) 1-13.
- [22] R. C. Houtz, *Text. Res. J.* 20 (1950) 786-801.
- [23] M. S. A. Rahaman, A. F. Ismail, A. Mustafa, *Polym. Degrad. Stabil.* 92 (2007) 1421-1432.
- [24] A. Ôya, H. Marsh, *J. Mater. Sci.* 17 (1982) 309-322.
- [25] P. Moravec, J. Smolík, H. Keskinen, J. M. Mäkelä, S. Bakardjieva, V. V. Levitskiy, *Mater. Sci. Appl.* 2 (2011) 258-264.
- [26] E. Zussman, X. Chen, W. Ding, L. Calabri, D. A. Dikin, J. P. Quintana, R. S. Ruoff, *Carbon* 43 (2005) 2175-2185.
- [27] W. F. Smith, J. Hashemi, *Foundations of materials science and engineering*, McGraw-Hill, 2003.
- [28] M. S. Dresselhaus, G. Dresselhaus, K. Sugihara, I. L. Spain, H. A. Goldberg, *Graphite fibers and filaments*, Springer Verlag, Berlin, 1988.
- [29] A. M. Bazargan, S. Ghashghai, M. Keyanpour-rad, M. Esmailpour Ganji, *RSC Adv.* 2 (2012) 1842-1845.
- [30] A. B. Garcia, I. Camean, I. Suelves, J. L. Pinilla, M. J. Lazaro, J. M. Palacios, R. Moliner, *Carbon* 47 (2009) 2563-2570.

#### AUTHOR (S) BIOSKETCHES

**Bazargan, A.M.**, PhD Candidate, Department of Polymer Engineering and Color Technology, Amirkabir University of Technology, 15875-4413 Tehran, Iran. Email: [ambazargan@gmail.com](mailto:ambazargan@gmail.com)

**Esmailpour, M.**, PhD, Department of Materials Engineering, Isfahan University of Technology (IUT), Isfahan, 84156-83111, Iran. Email: [maryam.esmailpour@gmail.com](mailto:maryam.esmailpour@gmail.com)

**Keyanpour-rad, M.**, Ph.D., Professor, Materials and Energy Research Center, P. O. Box 14155-4777, Tehran, Iran. E-mail: [m.kianpour@gmail.com](mailto:m.kianpour@gmail.com)

#### How to cite this article:

*Bazargan A.M, Esmailpour M, Keyanpour-Rad M. Catalytically Graphitized Electrospun Carbon Nanofibers Adorned with Nickel Nanoparticles for Catalysis Applications. J. Nanostruct.*2016; 6(1):52-57.

DOI: 10.7508/jns.2016.01.008

URL: [http://jns.kashanu.ac.ir/article\\_13642.html](http://jns.kashanu.ac.ir/article_13642.html)